INL/JOU-24-77237-Revision-0

Evaluation of U10Mo Fuel Plate Performance modeling over Hot Isostatic Press and Hydraulic Bending for MURR-DDE Plates

September 2025

Changing the World's Energy Future

Jason L Schulthess, Hakan Ozaltun, Kyle Mitchell Paaren, Jason Wayne Barney

Idaho National Laboratory

INL is a U.S. Department of Energy National Laboratory operated by Battelle Energy Alliance, LLC

INL/JOU-24-77237-Revision-0

Evaluation of U10Mo Fuel Plate Performance modeling over Hot Isostatic Press and Hydraulic Bending for MURR-DDE Plates

Jason L Schulthess, Hakan Ozaltun, Kyle Mitchell Paaren, Jason Wayne Barney

September 2025

Idaho National Laboratory
Idaho Falls, Idaho 83415

http://www.inl.gov

Prepared for the
U.S. Department of Energy
Under DOE Idaho Operations Office
Contract DE-AC07-05ID14517

Evaluation of U10Mo Fuel Plate Performance Modeling over Hot Isostatic Press and Hydraulic Bending for MURR DDE Plates

Kyle M. Paaren* (kyle.paaren@inl.gov), Jason Schulthess (Jason.schulthess@inl.gov), Jason Barney (Jason Barney@inl.gov), and Hakan Ozaltun (hxo@nrc.gov)

Idaho National Laboratory: 2525 Fremont Ave. Idaho Falls, Idaho, 83415

*Corresponding Author

KEYWORDS
ABAQUS
Simulation
Plasticity
HIP
Metallic Fuel

FIGURES
All Figures need to be in color.

ABBREVIATIONS
ATR — Advanced Test Reactor
DDE — Design Demonstration Elements
FSP1 — Full-Size Plate 1
HIP — Hot Isostatic Pressing
HPRR — High Performance Research Reactor
MP1 — Mini Plate 1
MP2 — Mini Plate 2
MURR — Missouri University Research Reactor

ABSRACT

The United States High Performance Research Reactor Program's objective is to reduce the amount of highly enriched uranium currently implemented in research reactors. The conversion of these research reactors requires designing a monolithic U10Mo plate fuel, with the fuel plate geometry being dependent on each research reactor. The process of forming the plates includes a hot isostatic pressing to manufacture a prototypic plate. In the case of the Missouri University Research Reactor (MURR) design demonstration elements (DDE) plate manufacture, plates that have been though hot isostatic pressing are then curved using dies and a hydraulic press to impart the desired curvature. Both fabrication processes impart residual stresses into each fuel plate region, with the curvature of the plates taking some regions of the fuel plate up to their material yield stresses, accompanied by plastic strain. The amount of plastic strain and stress imparted onto each MURR DDE plate is determined by the radius of curvature, thickness of each region, and overall width of the fuel plates. This work aims to predict the yield stresses and strain using ABAQUS to simulate the proposed fabrication process of the MURR DDE plates, accompanied by discussion over the stresses and strains as to their relation to nuclear fuel performance and the impact they will have during early irradiation.

INTRODUCTION

Within the United States High Performance Research Reactor Program, there is an ongoing effort to reduce the amount of highly enriched uranium used in research reactors. The development of lower enriched fuels requires a significant amount of design and fabrication choices to meet linear heat generation rates while meeting operational safety requirements. An alloy of U and Mo in the cubic γ phase has been selected as the fuel of choice for reactor conversion due to its preferred irradiation behavior and previous successful experiments [1]. There are two different types of U-Mo plate fuel, dispersion and monolithic, with the latter being alloyed at approximately 10wt% Mo and being used for high performance research reactor (HPRR) conversion due to the increased fuel density [1]. The mechanical response of the plates during irradiation conditions, as well as fabrication methods, needs to be well described and documented. Within this manuscript, the modeling of the fabrication process will be discussed, as the residual stresses and displacements of the plates may impact early fuel performance, irradiation behavior, and possible fuel failure.

For the monolithic plates, there are several steps for complete fabrication. These include casting, zirconium plating, hot rolling, cold rolling, annealing, shearing, and finally bonding the U10Mo fuel between two sections of Al6061 cladding via hot isostatic pressing (HIP) [2]. U10Mo feedstock is cast in a vacuum atmosphere in the form of coupons and then overlaid with a zirconium foil before being inserted into a rolling canister. The canister is then heated to 923 K before being hot rolled to a thickness of 0.5 mm. After the U10Mo fuel is removed from the canister, the foil is cold rolled to the appropriate thickness specified within the technical drawings [3-5]. Cold rolling allows for the U10Mo fuel to be hardened by introducing dislocations, increasing the modulus of elasticity. By annealing the U10Mo cold-rolled foils, the stress within the fuel is reduced and residual stresses decreased [2]. Within in this work and prior works within the HPRR program, it is assumed that annealing removes all residual stresses caused by the casting and cold rolling before the HIP is performed.

Before the HIP occurs, one side of the cladding is milled away to create a pocket for the U10Mo foil. Another section of Al6061 cladding is positioned over the fuel and then placed within the HIP canister. The canister or HIP can is then seal welded while under vacuum. The sealed canister is then placed into a hot isostatic press where inert gas is passed into the press and then heated to a temperature of 833 K at a pressure of 104 MPa. This temperature is important, as the Al6061 cladding is above its solution temperature of 802 K and below its solidus temperature of 855 K [6]. After a holding period of 90 minutes, it is assumed that the formed plate is cooled to room temperature (294 K) over 117 minutes [7]. The residual stresses incurred from the HIP process are later relieved under initial irradiation conditions due to creep [8, 9]. For most of the plates within the HPRR program, this is where the fabrication process ends. In the case of plates designated for the experiment known as Missouri University Research Reactor (MURR) Design Demonstration Elements (DDE) and other curved plates, a hydraulic press induces a plate curvature. Figures 1-2 show the geometry of these plates.

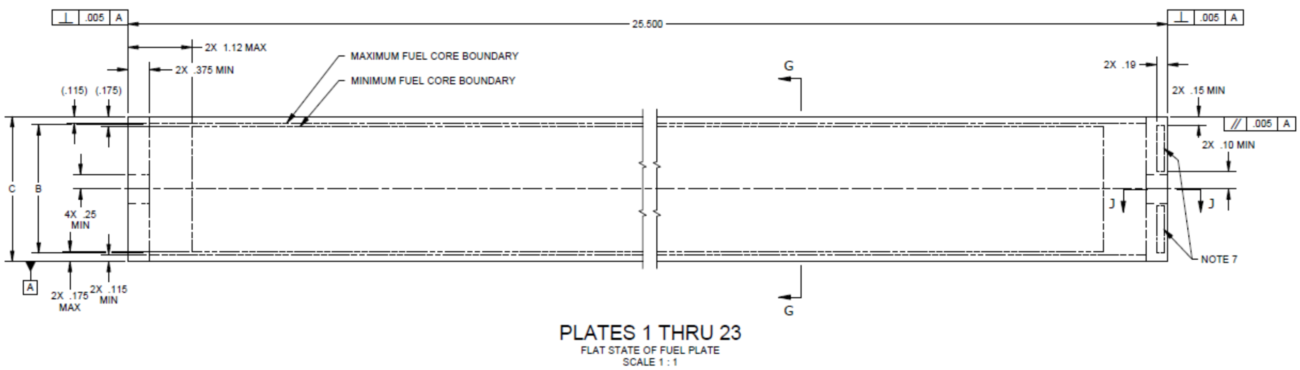

Figure 1. Front View of MURR DDE Plates 1–23

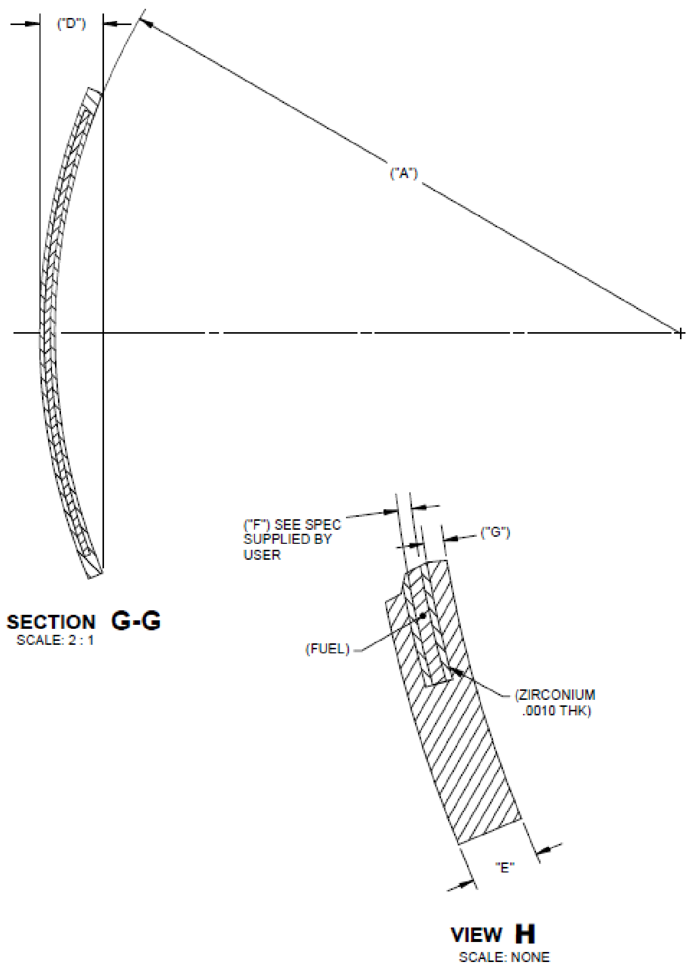

Figure 2. Cross Section of MURR DDE Plates 1–23

For the MURR DDE plates in this work, each of the 23 plates underwent the conditions outlined above, in addition to curving the plates by using a hydraulic press. For each of the plates, the specified radius is achieved by using die presses at room temperature. Table 1 lists the MURR DDE plates being fabricated with their corresponding end dimensions. This process requires the plates to be taken past their as-designed displacements due to the removal of elastic strain when the stress is released [10]. The final plate dimensions are achieved by the plastic strain created within the fuel and cladding, with residual stresses being at material yield stresses before irradiation. The calculated plastic strain for each plate obtained from ABAQUS is presented in this work, along with a discussion over the impact of residual stresses on fuel performance under irradiation.

Table 1. MURR DDE Plate Dimensions

Plate No.	Curvature Radius (A, mm)	Fuel Width (B, mm)	Plate width (C, mm)	Plate Deflection (D, mm)	Plate thickness (E, mm)	Fuel thickness (F, mm)	Al thickness (G, mm)
1	69.99	42.93	50.29	5.51	1.12	0.23	0.42
2	73.47	45.64	53.01	5.77	1.12	0.30	0.38
3	76.95	48.39	55.75	6.05	1.12	0.41	0.33
4	80.43	51.10	58.47	6.30	1.12	0.51	0.28
5	83.91	53.85	61.21	6.58	1.12	0.51	0.28
6	87.36	56.57	63.93	6.83	1.12	0.51	0.28
7	90.82	59.28	66.65	7.09	1.12	0.51	0.28

8	94.27	61.98	69.34	7.34	1.12	0.51	0.28
9	97.73	64.69	72.06	7.62	1.12	0.51	0.28
10	101.18	67.41	74.78	7.87	1.12	0.51	0.28
11	104.64	70.13	77.50	8.13	1.12	0.51	0.28
12	108.09	72.85	80.21	8.41	1.12	0.51	0.28
13	111.54	75.54	82.91	8.66	1.12	0.51	0.28
14	115.00	78.26	85.62	8.92	1.12	0.51	0.28
15	118.45	80.98	88.34	9.19	1.12	0.51	0.28
16	121.91	83.69	91.06	9.45	1.12	0.51	0.28
17	125.36	86.41	93.78	9.70	1.12	0.51	0.28
18	128.82	89.10	96.47	9.96	1.12	0.51	0.28
19	132.27	91.82	99.19	10.24	1.12	0.51	0.28
20	135.75	94.56	101.93	10.49	1.12	0.51	0.28
21	139.23	97.28	104.65	10.77	1.12	0.51	0.28
22	142.71	100.03	107.39	11.02	1.12	0.51	0.28
23	146.19	102.82	110.19	11.43	1.24	0.43	0.38

METHODS

The ABAQUS simulations performed for the MURR DDE plates within this work utilized version 2021HF6, which has been shown to be thermal mechanically equivalent to ABAQUS 6.14-2, where the majority of the modeling and simulation work has been done for the Reduced Enrichment for Research and Test Reactors and HPRR Programs [11-15]. Each simulation consisted of a MURR DDE plate utilizing as-designed dimensions and tolerances, using C3D8RTI elements for thermal mechanical analyses. Utilizing the reduced-order, integrated elements allowed for better convergence compared to C3D8 elements without reduced integration, without volumetric locking occurring. This is consistent with previous modeling techniques for the fuel plates [11-15]. The general model setup for the MURR DDE plates is discussed in this work, along with the relevant material properties used to predict plastic deformation.

General Solution

All ABAQUS simulations used in this work are based on previous HIP conditions used to model the Mini Plate 1 (MP1), Mini Plate 2 (MP2), and Full-Size Plate 1 (FSP1) plates for the HPRR Program, with the addition of a displacement field added after the HIP step to apply curvature to the MURR DDE plates [12, 13, 15]. As previously mentioned, C3D8RTI elements were utilized, with a global base size of 0.45 mm, with each section of fuel, cladding, and zirconium layer containing three elements. Three elements per layer were chosen to adequately represent the stress and strains between each layer for the fuel plate. This mesh base size and edge seeding yielded an average aspect ratio of 4.883. Each section of the fuel plate was created using datum planes, with the offsets adjusted to the as-designed dimensions. The mesh of Plate 1 is shown in Figure 3. Section assignments were then created for the U10Mo fuel, zirconium layer, and Al6061 cladding, with the appropriate materials assigned to each.

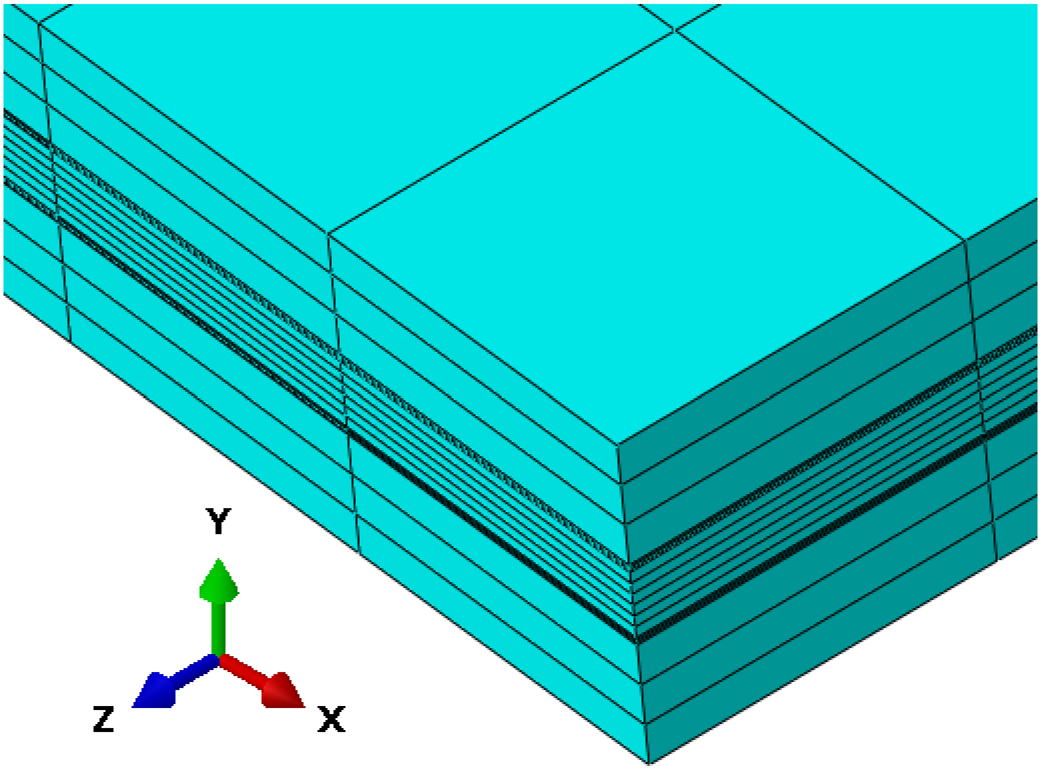

Figure 3. Corner Mesh of MURR DDE Plate 1

The material properties utilized for U10Mo monolithic fuel, zirconium liner, and Al6061 include thermal conductivity, specific heat, thermal expansion, thermal creep, density, elastic, and plastic properties as a function of temperature [16-20]. The inclusion of each of these material properties is important to accurately model the stress and strain states within the fuel plates during the manufacturing process, with all the material properties assumed to be isotropic. The material properties used within these ABAQUS simulations have been documented elsewhere within the HPRR Program, prior works, and recently within the BISON fuel performance code [16-20]. Out of all the material properties within the modeling work, the most important to be included in this work is plasticity, as ignoring this mechanism would only allow plasticity to come from creep. This is important to account for when modeling plate curvature, as not doing so would produce unrealistic stresses in the simulations.

Several boundary conditions were used for the ABAQUS fuel plates, which include fixing all surfaces on axial lines of symmetry with Dirichlet conditions. This sets the corresponding displacements to zero at those surfaces so no elastic or inelastic eigenstrains occurred over the axial boundary line. Doing so along the x, y, and z centerlines of the fuel plate allows for a reference point to be established for swelling deformation. For the interface between the U10Mo fuel, zirconium, and Al6061 cladding, it is assumed that each layer is bonded together, such that delamination due to stress cannot occur. This is a justified assumption, as the fabrication process being modeled is HIP. For future work, a determined bond strength will be used based on HIP temperature, time, and precipitate microstructure to be switched from glued mechanical contact to a frictionless interface for nodes that exceed that particular von Mises stress [7].

For simulating the fabrication process, two steps were constructed within the ABAQUS simulations. The first step includes taking each plate from an initial temperature of 833 K down to room temperature (294 K) linearly over 117 minutes. The HIP duration was chosen due to it being documented in prior works [7]. This decrease in temperature under an initial 104 MPa of pressure resulted in residual stress states prior to the hydraulic bending of the plates. This is important to capture, as less energy is needed to form the plate to the desired curvature due to the plates containing preloaded stress. Modeling the HIP fabrication will also lead to higher plastic deformation within the fuel and cladding.

The second step modeled within ABAQUS applied an analytical field to the displacements along the width of the plate (x-axis) to force a plate curvature. The analytical field involved constructing an equation for a circle with the given radius in Table 1 as a function of distance along the width of the plate (x-axis). By forcing the displacements, ABAQUS uses solid mechanics to solve for the equivalent stresses and plastic strains necessary to achieve each plate curvature. This was done for each of the 23 MURR DDE plates due to variations in curvature, fuel, and cladding thickness. Figure 4 shows a visualization of the curvature displacement boundary condition.

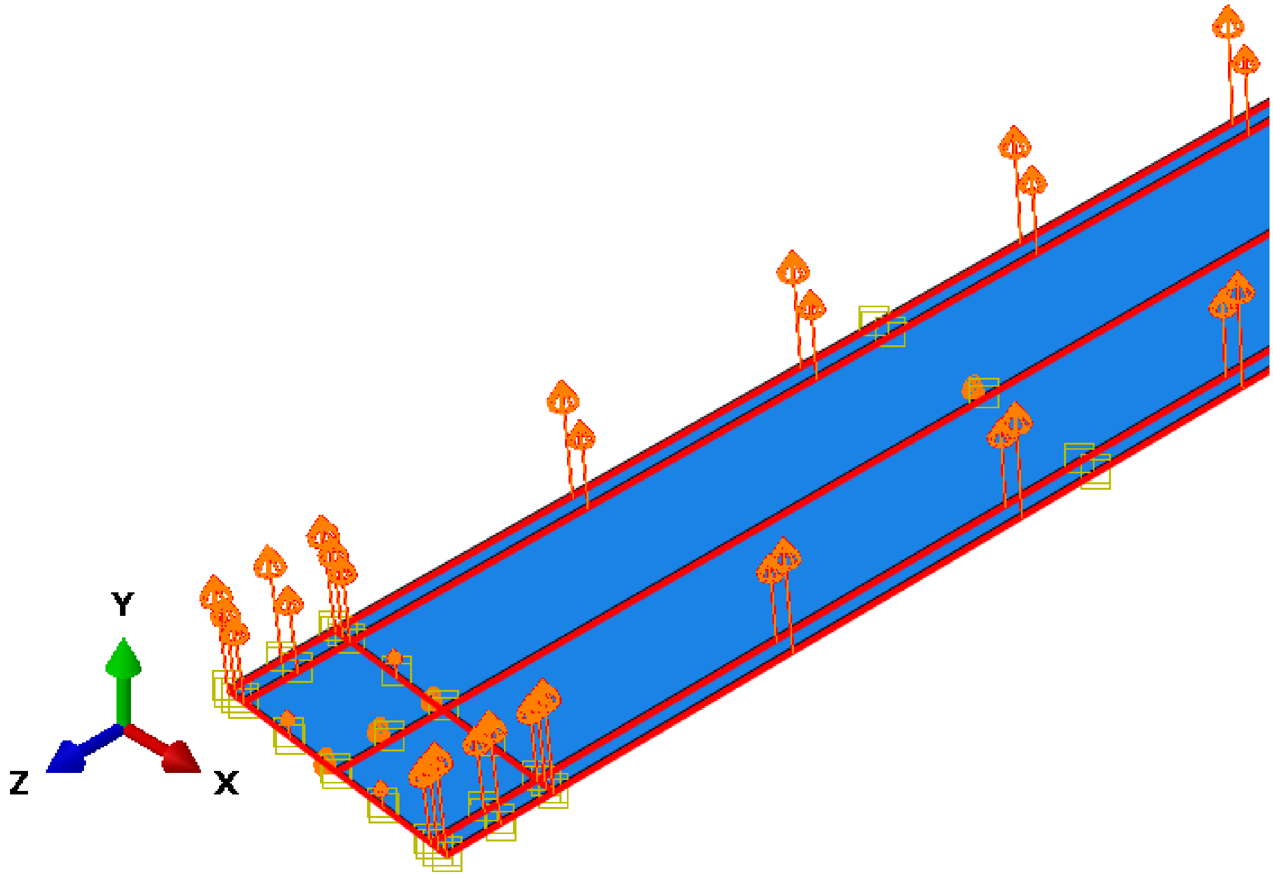

Figure 4. Displacement boundary condition to replicate curvature of MURR DDE Plates 1–23

RESULTS

To illustrate the ABAQUS simulations, both the HIP and curvature of all 23 MURR DDE plates are shown and discussed in this section to inform fabrication of potential issues with bond strength and fuel fatigue from plastic deformation. Cladding stresses presented within these sections were well below the yield stresses for Al6061. Within the curvature simulations, all 23 plates experienced plastic deformation within the U10Mo fuel, zirconium liner, and Al6061 cladding. The plate with the largest plastic strain was MURR DDE Plate 2, due to the tight plate curvature and increased fuel thickness.

HOT ISOSTATIC PRESSING

Within the fabrication process of the MURR DDE plates, HIP was simulated within ABAQUS using 117 minutes of cooling time from 833 K to room temperature [7]. This temperature swing allowed for residual stress within the fuel and cladding to build up within the U10Mo monolithic fuel plate, with plates with thinner fuel thickness experiencing higher residual stresses within the fuel, such as MURR DDE Plates 1 and 23. This is due to the difference in thermal expansion coefficients between Al6061 and the fuel. Maximum residual stresses within the zirconium and Al6061 cladding were shown to be consistent, with the thickness of the cladding and fuel regions having no impact. The maximum stresses within the fuel region occurred on the edge boundary, along the width of the plates. The maximum stresses for the zirconium and Al6061 cladding occurred on the faces parallel to the surfaces of the fuel foil. Table 2 lists the maximum von Mises stresses and creep strain for each plate. Thermal creep for Al6061 cladding and the zirconium liner were included in the HIP analysis due to the starting temperature of the HIP process. Thermal creep was not included for the fuel region due to the insignificant impact it had on displacements and model convergence.

Table 2. Element Average MURR DDE HIP Von Mises Stress (MPa, left) and Thermal Creep Strain CEEQ (right)

Plate No.	Fuel	Zr	Cladding	Zr	Cladding
1	305.6	323.9	62.85	8.27E-05	3.71E-03
2	254.6	323.4	64.01	8.27E-05	4.12E-03
3	210.1	322.9	65.53	8.27E-05	4.20E-03
4	190.3	322.6	66.59	8.27E-05	4.80E-03
5	192.3	322.7	66.65	8.27E-05	4.84E-03
6	194.2	322.7	66.72	8.27E-05	4.87E-03
7	196.2	322.7	66.77	8.27E-05	4.90E-03
8	198.1	322.8	66.81	8.27E-05	4.93E-03
9	199.8	322.9	66.85	8.27E-05	4.97E-03
10	201.5	322.7	66.89	8.27E-05	4.99E-03
11	203.0	322.7	66.93	8.27E-05	5.02E-03
12	204.4	322.7	66.97	8.27E-05	5.05E-03
13	205.7	322.7	67.01	8.27E-05	5.07E-03
14	207.2	322.7	67.05	8.27E-05	5.09E-03
15	208.3	322.7	67.09	8.27E-05	5.11E-03
16	209.3	322.7	67.13	8.27E-05	5.13E-03
17	210.1	322.7	67.17	8.27E-05	5.15E-03
18	210.9	322.7	67.21	8.27E-05	5.16E-03
19	211.6	322.7	67.25	8.27E-05	5.17E-03
20	212.2	322.7	67.29	8.27E-05	5.18E-03
21	212.8	322.7	67.33	8.27E-05	5.19E-03
22	213.2	322.7	67.37	8.27E-05	5.19E-03
23	228.9	322.7	66.56	8.27E-05	4.61E-03

The small amount of plastic deformation occurring within the Al6061 cladding and the zirconium liner is due to the negative thermal expansion, with the Al6061 cladding wanting to uniformly contract and compress around the fuel and zirconium liner. The plastic strain for the zirconium liner was significantly less than the Al6061 cladding due to differences in material properties and thickness, as seen in Table 3 and Figure 5. Von Mises stresses within the cladding follow a similar profile to that of the plastic strain shown in Figure 5. The decrease in plastic strain through the HIP process for Plates 1–4 is explained by the increase in fuel thickness, with there being less Al6061 cladding material.

Table 3. Element Average MURR DDE HIP Elastic Strain EE (left) and Plastic Strain PEEQ (right)

Plate No.	Fuel	Zr	Cladding	Zr	Cladding
1	2.82E-03	2.44E-03	8.82E-04	1.09E-02	2.55E-02
2	2.03E-03	2.44E-03	8.92E-04	9.92E-03	2.97E-03
3	1.56E-03	2.46E-03	9.04E-04	9.07E-03	3.55E-03
4	1.39E-03	2.48E-03	9.22E-04	8.55E-03	3.97E-03
5	1.42E-03	2.48E-03	9.25E-04	8.54E-03	4.00E-03
6	1.46E-03	2.48E-03	9.27E-04	8.54E-03	4.03E-03
7	1.48E-03	2.48E-03	9.29E-04	8.52E-03	4.04E-03
8	1.51E-03	2.47E-03	9.31E-03	8.51E-03	4.06E-03

9	1.53E-03	2.47E-03	9.36E-04	8.50E-03	4.08E-03
10	1.56E-03	2.47E-03	9.43E-04	8.49E-03	4.09E-03
11	1.58E-03	2.47E-03	9.48E-04	8.48E-03	4.10E-03
12	1.60E-03	2.46E-03	9.54E-04	8.47E-03	4.12E-03
13	1.61E-03	2.46E-03	9.59E-04	8.46E-03	4.13E-03
14	1.63E-03	2.46E-03	9.63E-04	8.46E-03	4.15E-03
15	1.65E-03	2.46E-03	9.68E-04	8.45E-03	4.16E-03
16	1.66E-03	2.46E-03	9.71E-04	8.44E-03	4.17E-03
17	1.68E-03	2.46E-03	9.75E-04	8.44E-03	4.18E-03
18	1.69E-03	2.48E-03	9.78E-04	8.43E-03	4.19E-03
19	1.70E-03	2.46E-03	9.80E-04	8.43E-03	4.19E-03
20	1.71E-03	2.46E-03	9.83E-04	8.42E-03	4.20E-03
21	1.72E-03	2.46E-03	9.85E-04	8.43E-03	4.21E-03
22	1.72E-03	2.46E-03	9.86E-04	8.43E-03	4.22E-03
23	1.61E-03	2.44E-03	9.51E-04	8.72E-03	3.96E-03

It is expected that no plastic strain occurs at the edge of the Al6061 cladding, as there is no fuel or zirconium liner beneath it and it has a constant thermal expansion. The elastic strain for the Al6061 cladding peaks and increases around the boundary of the fuel and zirconium liner, as it has not yet been transitioned to plastic strain and is where the maximum von Mises stress occurs. A similar trend is seen in the fuel region, where elastic strain occurs where the maximum von Mises stress is found.

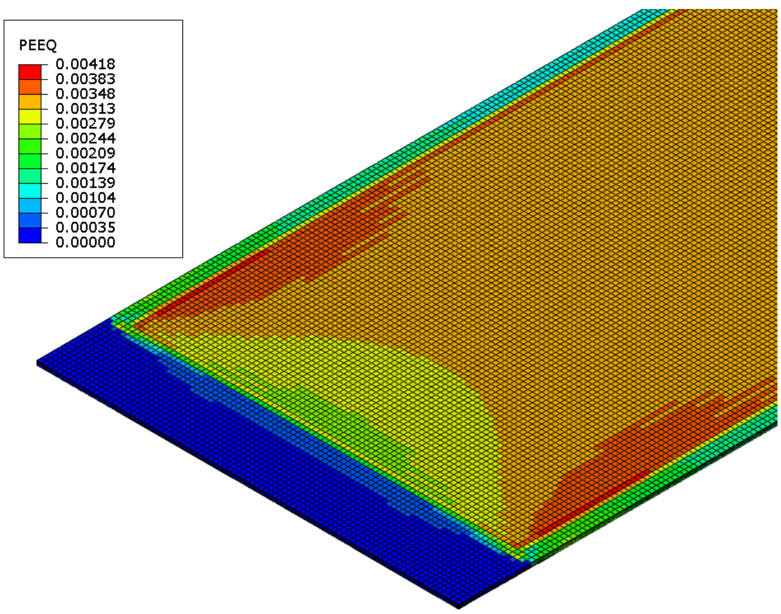

Figure 5. MURR DDE HIP Cladding Plastic Strain (PEEQ)

CURVATURE OF PLATES

After HIP is performed on the MURR DDE plates, the corresponding displacements listed in Table 1 were supplied to the edges of each of the MURR DDE plates. By forcing the displacements to occur within ABAQUS, solid mechanics are used to solve the equivalent stresses and plastic strains necessary to achieve the needed curvature. Creep strain for the zirconium liner and Al6061 cladding were not reported for plate curvature, as the process occurred at room temperature, and no additional thermal creep occurred. Elastic strain for the MURR DDE plates after the curvature was complete was not reported, as the plastic strain from the plate curvature was magnitudes higher and is the primary focus of this work.

In all of the 23 MURR DDE plates, the yield stress for the fuel, zirconium liner, and Al6061 was reached in each orientation. Due to the limited plastic strain data available for U10Mo fuel, it was assumed that the material is perfectly plastic after the yield stress is exceeded, as shown in Table 4, with the maximum stress within the fuel region being 996 MPa. It should be noted that MURR DDE Plates 1–4 had subsequently increased fuel thickness, with the curvature radius also decreasing. This leads to a slight increase in plastic strain for Plate 2, with a decrease in plasticity as the radius of curvature is increased in Plate 3. Plates 4–22 had the same fuel thickness, with the curvature radius decreasing, and the oval width of the plates increasing. Plate 23 has a similar fuel thickness to Plate 3, which allowed for less plastic strain to occur within the fuel region, consequently allowing the Al6061 cladding to deform more, which is shown in Figure 6.

Table 4. Element Average MURR DDE Curvature Von Mises Stress (MPa, left) and Plastic Strain PEEQ (right)

Plate No.	Fuel	Zr	Cladding	Fuel	Zr	Cladding
1	996	392.0	156.1	0.05113	0.04930	0.1157
2	996	418.6	161.0	0.07963	0.07592	0.1373
3	996	411.3	158.8	0.07406	0.06801	0.1289
4	996	412.6	158.5	0.07741	0.06939	0.128
5	996	413.6	158.5	0.07838	0.07051	0.1282
6	996	414.7	158.6	0.07973	0.07164	0.1284
7	996	415.5	158.6	0.08064	0.07257	0.1285
8	996	416.3	158.8	0.0814	0.07344	0.1286
9	996	417.1	159.0	0.08219	0.07426	0.1287
10	996	417.8	159.2	0.08291	0.07509	0.1289
11	996	418.5	159.4	0.08362	0.07583	0.129
12	996	419.2	159.6	0.08427	0.07657	0.1291
13	996	419.7	159.8	0.08485	0.07718	0.1292
14	996	420.4	160.1	0.0857	0.07791	0.1293
15	996	421.0	159.5	0.08635	0.07859	0.1294
16	996	421.5	158.9	0.0868	0.07911	0.1295
17	996	422.0	158.6	0.08725	0.07963	0.1296
18	996	422.5	158.9	0.0877	0.08015	0.1297
19	996	423.0	158.6	0.08815	0.08067	0.1297
20	996	423.4	158.6	0.08859	0.08116	0.1297
21	996	423.8	159.0	0.08927	0.08162	0.1298
22	996	424.3	158.6	0.08955	0.08209	0.1299
23	996	424.3	158.6	0.08834	0.08217	0.1306

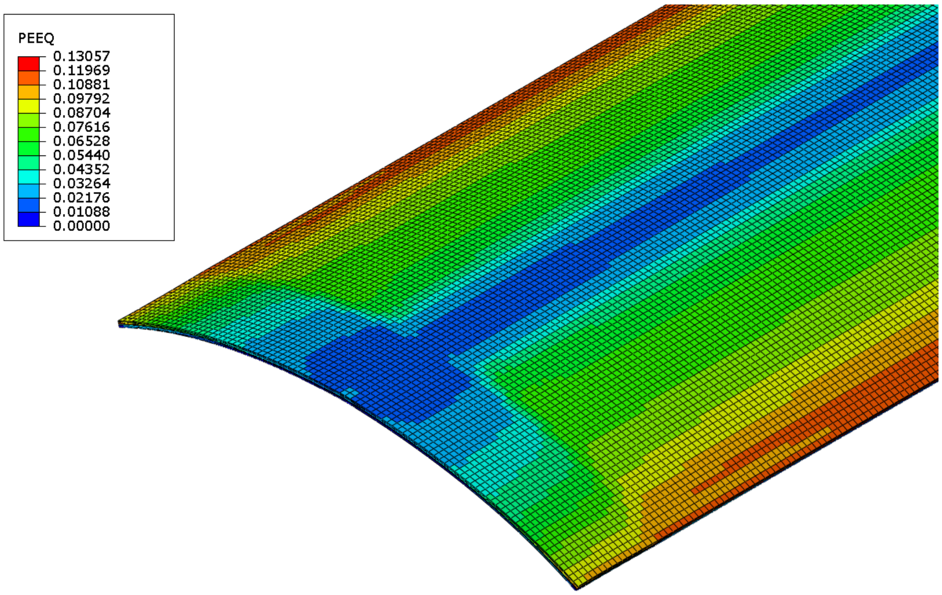

Figure 6. MURR DDE Curvature Cladding Plastic Strain Plate 23 (PEEQ)

Between Figures 6 and 7, the stresses and plastic strain profiles for each of the MURR DDE plates mirror each other and are uniform along the Z axis. The maximum von Mises and plastic strains occur along the plate edge of the Al6061 cladding, zirconium liner, and fuel, with the differences being their magnitudes. On the width edge of the plates, the Al6061 cladding has significantly less stress and reduced plastic strain due to no presence of fuel or zirconium liner.

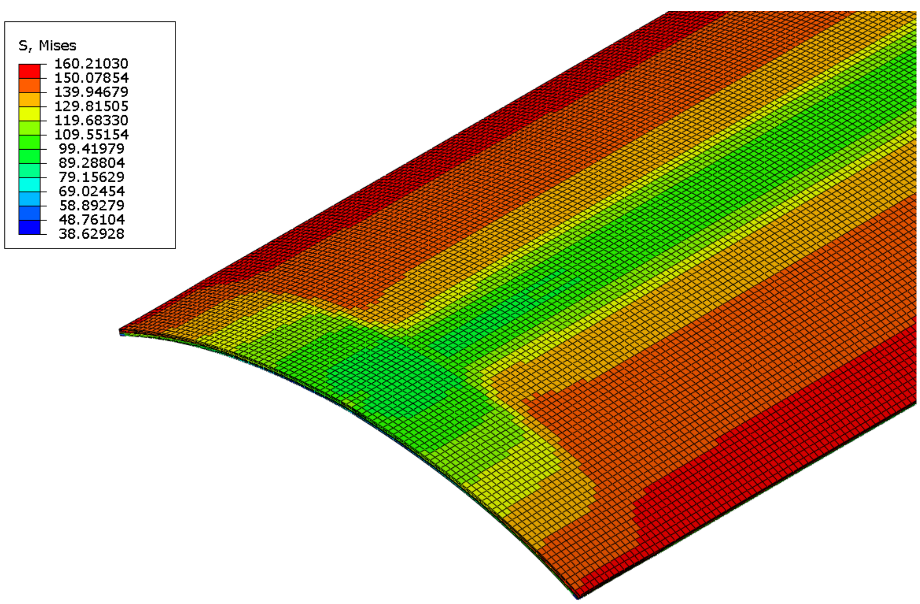

Figure 7. MURR DDE Curvature Cladding Von Mises Plate 23

DISCUSSION

The fabrication process of the MURR DDE plates incorporates a HIP process identical to other fuel plates used within the HPRR program, such as MP1, MP2, and FSP1. However, MURR DDE monolithic plates utilize an additional fabrication step involving a hydraulic press, a ram, and dies to property impart curvature to the plates at room temperature. In doing so, the residual stresses remaining after HIP are increased to yield stress levels, with plastic strain needed to impart and hold plate curvature after external pressure of the hydraulic press is released.

For previous fabrication of the plates within MP1, MP2, and FSP1, residual stresses were low enough that no annealing was performed on the monolithic plates before they entered Advanced Test Reactor (ATR) for irradiation [15]. The reason for the low stresses is due to the plates having the residual stresses reduced in the fuel and cladding by thermal creep under irradiation. Typically, stresses within the fuel creep down to ~20 MPa from their initial HIP residual stress values of ~200 MPa [21]. Relieving this stress causes creep strain within the fuel and the cladding, which will cause the monolithic plates to deform slightly on the outer plate surfaces, which is shown in an FSP1 plate in Figure 8.

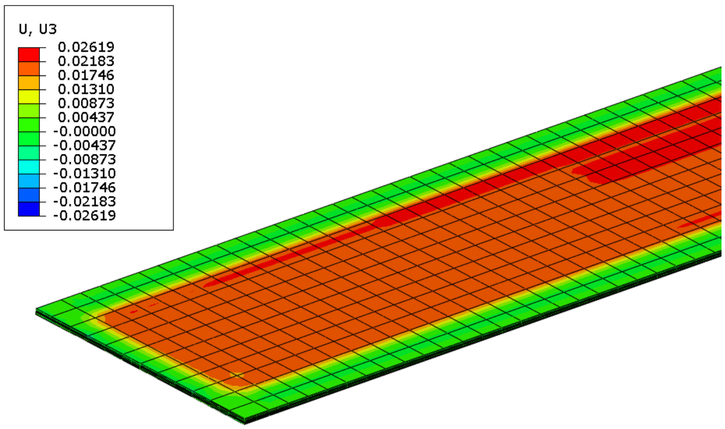

Figure 8. FSP-1 Full Burn Plate 1 Displacements after 60 Day Cycle

With the MURR DDE plates including plate curvature within their fabrication process and residual stresses being significantly higher in the U10Mo, zirconium liner, and Al6061 cladding than in previous plates, there is concern around the deformation of the MURR DDE plates once irradiation was to occur once residual stresses are relieved. The MURR DDE plates are planned to be swaged and held by the edge of the plates, as denoted in Figure 9. Due to the proposed pressure differential on each side of the plates and the linear heat generation rates distribution on each plate, both parameters, along with the built-up residual stresses, will deform the plates and contribute to fuel performance.

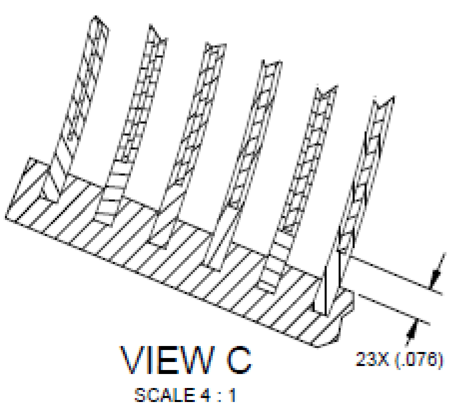

Figure 9. Swaging of MURR DDE Plates

Within the HPRR program, an additional fabrication step is planned beyond plate curvature to anneal some of the MURR DDE test plates to measure the amount of deflection that would occur from the removal of residual stresses. Currently, the fabrication of the MURR DDE plates is planned for June 2026–January 2028, and the as-planned neutronic and thermal analyses has not yet been performed to transfer over to the steady-state fuel performance simulations. Depending on irradiation experiment limitations of channel gap thicknesses, annealing the MURR DDE plates may be unnecessary. Plate deformation under irradiation conditions, and the release of residual stresses, may be within design limits without additional annealing.

CONCLUSIONS

The fabrication process of the MURR DDE plates were successfully modeled within ABAQUS, including the HIP and curvature of the plates, for all 23 plates to be irradiated within ATR. Within the ABAQUS simulations, Plate 1 with the thinnest U10Mo fuel section showed the highest residual stresses out of the 23 plates. This is due to the thicker Al6061 cladding wanting to uniformly contract and compress around the fuel. The location of the high residual stress within the fuel and the cladding were along the width edge of each fuel plate. Which was expected due to the location of the material zones and the difference in material properties. The curvature of the plates leads to interesting results, as the fuel thickness, curvature radius, and the overall width of the plate had an impact on the residual stress and plastic strain within the U10Mo fuel, zirconium layer, and Al6061 cladding. MURR DDE Plate 2 obtained the highest plastic strain within the 23 plates due to the thick fuel region and higher radius of curvature. Plate 23, although having a lower fuel thickness than Plates 4–22, achieved the second highest plastic strain within the Al6061 cladding and the highest plastic strain within the zirconium liner. In all cases, the peak plastic strain for each of the plates occurred at the outer edge similar to FSP1, as shown in Figure 6. In each curvature simulation, the yield stress within the fuel was obtained, being 996 MPa for room temperature. Due to the amount of residual stress built up within the MURR DDE monolithic plates during fabrication, the possibility of annealing is being considered. Once neutronics and thermal hydraulics calculations for the proposed irradiations are available, a scoping study will assess the fuel performance of the irradiation and whether annealing the MURR DDE plates is necessary. The fuel performance predictions of the MURR DDE plates in early irradiation will determine channel gaps predictions before ATR irradiations begin.

ACKNOWLEDGEMENTS

The authors acknowledge Adam X. Zabriskie, Stephen R. Novascone, Nancy J. Lybeck, Aaron Oaks, Kun Mo, and Abdellatif Yacout for providing review input, knowledge, and experimental data.

This manuscript has been authored by Battelle Energy Alliance, LLC under Contract No. DE-AC07-05ID14517 with the U.S. Department of Energy. The U.S. Government retains and the publisher, by accepting the article for publication, acknowledges that the U.S. Government retains a nonexclusive, paid-up, irrevocable, world-wide license to publish or reproduce the published form of this manuscript, or allow others to do so, for U.S. Government purposes.

This research made use of Idaho National Laboratory's High Performance Computing systems located at the Collaborative Computing Center and supported by the Office of Nuclear Energy of the U.S. Department of Energy and the Nuclear Science User Facilities under Contract No. DE-AC07-05ID14517.

REFERENCES

[1] G. L. H. J. L. Snelgrove, M. K. Meyer, C. L. Trybus and a. T. C. Wienceck, "Development of Very-High Density Low Enriched Uranium Fuels," *Journal of Nulcear Engineering and Design,* vol. 179, pp. 119-126, 1997.

[2] F. J. R. G. A. Moore, N. E. Woolstenhulme, J. Jue and B. and H. Park, "Monolithic Fuel Fabrication Process Development at the Idaho National Laboratory," presented at the RERTR 2009, Beijing, China, 2009, 2009.

[3] R. W. Briggs, C. R. Clark, and N. P. Hallinan, *RERTR-6 Fuel Plate Irradiation Experiments in the Adanced Test Reactor,* 2005.

[4] J. M. Beeston, R. R. Hobbins, G. W. Gibson, and W. C. Francis, "DEVELOPMENT AND IRRADIATON PERFORMANCE OF URANIUM ALUMINIDE FUELS IN TEST REACTORS," *Nuclear Technology,* vol. 49, no. 1, pp. 136-149, 1980, doi: 10.13182/NT80-A32515.

[5] A. A. Becker, T. H. Hyde, and L. Xia, "Numerical analysis of creep in components," *Journal of Strain Analysis for Engineering Design,* vol. 29, no. 3, pp. 185-192, 1994, doi: 10.1243/03093247V293185.

[6] G. H. a. M. L. T. Totev, "AA-Matpro - Handbook (Aluminum Materials Properties for Research Reactors)," Argonne National Laboratory, 2009 2009.

[7] H. P. B. J. F. Jue, R. C. Curtis, A. M. Glenn and D. K. Dennis, "Fabrication of monolithic RERTR fuels by HIP," *Journal of Nuclear Technology,* vol. 172, no. 2, pp. 204-210, 2010 2010.

[8] D. J. Alexander, K. D. Clarke, C. Liu, and M. L. Lovato, "Tensile properties of 6061 aluminum alloy materials," *Los Alamos National LAboratory Report LA-UR-11-06707,* 2011.

[9] "Rate-dependent plasticity: Creep and swelling," *ABAQUS Theory Manual,* 2010.

[10] N. E. W. R. B. N. M. H. S. G. K. Housley, "DDE-MURR Status Report of Conceptual Design Activities," Idaho National Laboratory, Idaho National Laboratory, 2013 2013.

[11] H. Ozaltun, H. Shen, and P. Medvedev, "Computational evaluation for the mechanical behavior for u10mo fuel miniplates subject to thermal cycling," *J. Nucl. Eng. des,* 2012.

[12] H. Ozaltun, H. Shen, and P. Medvedev, "Numerical simulation for mechanical behavior of u10mo monolithic miniplates," *IMECE2011,* 2011.
[13] H. Ozaltun and S. J. Miller, "Finite element simulations of monolithic plates for the conversion of high performance research and test reactors: NBSR, MITR, MURR and AFIP," in *ASME International Mechanical Engineering Congress and Exposition, Proceedings (IMECE)*, 2012, vol. 6, PARTS A AND B ed., pp. 1301-1321, doi: 10.1115/IMECE2012-89011.
[14] H. Ozaltun and S. J. Miller, "Evaluation of blister behavior for U10MO mini fuel plates with cold rolled foils," in *ASME International Mechanical Engineering Congress and Exposition, Proceedings (IMECE)*, 2012, vol. 6, PARTS A AND B ed., pp. 1337-1345, doi: 10.1115/IMECE2012-93141.
[15] H. Ozaltun, M. H. Herman Shen, and P. Medvedev, "Assessment of residual stresses on U10Mo alloy based monolithic mini-plates during Hot Isostatic Pressing," *Journal of Nuclear Materials,* vol. 419, no. 1-3, pp. 76-84, 2011, doi: 10.1016/j.jnucmat.2011.08.029.
[16] A. Karahan, "Modeling of thermo-mechanical and irradiation behavior of metallic and oxide fuels for sodium fast reactors," *Massachusetts Institute of Technology,* 2009.
[17] G. L. Hofman, Y. S. Kim, and A. B. Robinson, "Fission Induced Swelling and Creep of Uranium-Molybdenum Alloy Fuel," *Trans. 13th Intern. Topical Meeting on Research Reactor Fuel Management, RRFM 2009,* 2009.
[18] M. M. Hall Jr, "Stress state dependence of in-reactor creep and swelling. Part I: Continuum plasticity model," *Journal of Nuclear Materials,* vol. 396, no. 1, pp. 112-118, 2010, doi: 10.1016/j.jnucmat.2009.10.063.
[19] J. E. Gates, E. G. Bodine, J. C. Bell, A. A. Bauer, and G. D. Calkins, "Stress-strain Properties of Irradiated Uranium-10 W/O Molybdenum," *Stress-Strain Properties of Irradiated Uranium-10 W/o Molybdenum,* 1958.
[20] D. E. Burkes, R. Prabhakaran, T. Hartmann, J. F. Jue, and F. J. Rice, "Properties of DU-10 wt% Mo alloys subjected to various post-rolling heat treatments," *Nuclear Engineering and Design,* vol. 240, no. 6, pp. 1332-1339, 2010, doi: 10.1016/j.nucengdes.2010.02.008.
[21] J. B. K. M. Paaren, H. Ozaltun, P. G. Medvedev, "Thermal-Mechanical Displacement Analysis of the FSP-1 Experiment in the ATR NEFT Position," Idaho National Laboratory, Idaho National Laboratory, 2022.